Developmental Biology 321 (2008) 88–100

Contents lists available at ScienceDirect

Developmental Biology

journal homepage: www.elsevier.com/developmentalbiology

Rho GTPase controls invagination and cohesive migration of the *Drosophila* salivary gland through Crumbs and Rho-kinase

Na Xu [1], Benison Keung [2], Monn Monn Myat *

Department of Cell and Developmental Biology, Weill Medical College of Cornell University, 1300 York Avenue, New York, NY 10065, USA

ARTICLE INFO

Article history:
Received for publication 21 March 2008
Revised 28 May 2008
Accepted 3 June 2008
Available online 13 June 2008

Keywords:
Drosophila
Salivary
Gland
Invagination
Migration
Rho
Crumbs
Epithelia
Polarity
Tube

ABSTRACT

Coordinated cell movements shape simple epithelia into functional tissues and organs during embryogenesis. Regulators and effectors of the small GTPase Rho have been shown to be essential for epithelial morphogenesis in cell culture; however, the mechanism by which Rho GTPase and its downstream effectors control coordinated movement of epithelia in a developing tissue or organ is largely unknown. Here, we show that Rho1 GTPase activity is required for the invagination of *Drosophila* embryonic salivary gland epithelia and for directed migration of the internalized gland. We demonstrate that the absence of zygotic function of Rho1 results in the selective loss of the apical proteins, Crumbs (Crb), *Drosophila* atypical PKC and Stardust during gland invagination and that this is partially due to reduced *crb* RNA levels and apical localization. In parallel to regulation of *crb* RNA and protein, Rho1 activity also signals through Rho-kinase (Rok) to induce apical constriction and cell shape change during invagination. After invagination, Rho-Rok signaling is required again for the coordinated contraction and dorsal migration of the proximal half of the gland. We also show that Rho1 activity is required for proper development of the circular visceral mesoderm upon which the gland migrates. Our genetic and live-imaging analyses provide novel evidence that the proximal gland cells play an essential and active role in salivary gland migration that propels the entire gland to turn and migrate posteriorly.

Introduction

Epithelial cells move cohesively to form functional tissues and organs during embryogenesis. The specification of an epithelial placode followed by distinct changes in cell shape leading to the invagination of cells into the underlying tissue is a prevalent morphogenic movement observed during early stages of the formation of the lens and optic cup (Hilfer, 1983), otic vesicle (Alvarez and Navascues, 1990), neural tube (Schoenwolf and Smith, 1990), mammary gland, tooth and hair follicle (Mikkola and Millar, 2006). Similar changes in cell shape and movement are also observed in *Drosophila* and *Xenopus* gastrulation and *Drosophila* tracheal and salivary gland invagination (Hardin and Keller, 1988; Leptin, 1999; Myat, 2005). In addition to invagination, epithelial tissues and organs migrate as cohesive sheets or groups of cells. For example, *Drosophila* epidermal cells migrate as sheets during dorsal closure whereas border cells migrate as clusters of motile cells (Lecaudey and Gilmour, 2006). Despite the prevalence of epithelial invagination and migration in organogenesis, little is known about the molecular mechanisms that govern epithelial characteristics and movement.

Members of the Rho family of small GTPases are critical regulators of epithelial morphogenesis. They act as molecular switches to control epithelial cell polarity, cell–cell adhesion, cell–substratum adhesion and actin cytoskeleton organization (Jaffe and Hall, 2005). The small GTPase Rac has been shown to regulate cohesive movements of several epithelial tissues and organs in the *Drosophila* embryo such as dorsal closure migration (Woolner et al., 2005), tracheal cell rearrangement (Chihara et al., 2003) and salivary gland migration (Pirraglia et al., 2006). During *Drosophila* gastrulation, the small GTPase Rho signals through Myosin II to induce apical constriction and mediate invagination of mesodermal cells (Barrett et al., 1997; Nikolaidou and Barrett, 2004). Activators of Rho GTPase have also been shown to be required for invagination of the *Drosophila* embryonic salivary gland implicating Rho GTPase in this process (Kolesnikov and Beckendorf, 2007; Nikolaidou and Barrett, 2004); however, it is not known whether Rho GTPase controls salivary gland invagination solely through actin–myosin contraction or by multiple mechanisms.

Here, we analyze Rho GTPase function in morphogenesis of the *Drosophila* embryonic salivary glands. The salivary glands form by invagination of primordial cells from the embryo surface followed by cohesive migration of the gland along surrounding mesoderm (Myat, 2005). Gland cells invaginate by apical constriction and cell shape change from columnar to pyramidal, a process dependent on the

* Corresponding author. Fax: +1 212 746 8175.
E-mail address: mmm2005@med.cornell.edu (M.M. Myat).
[1] BCMB Program of Weill Graduate School of Medical Sciences at Cornell University, New York, NY, USA.
[2] Present address: New York Medical College, Valhalla, NY 10595, USA.

0012-1606/$ – see front matter © 2008 Elsevier Inc. All rights reserved.
doi:10.1016/j.ydbio.2008.06.007

transcription factor, Fork head (Fkh) (Myat and Andrew, 2000a; Myat and Andrew, 2000b). Hairy and Huckebein-dependent transcriptional regulation of the apical determinant protein, Crumbs (Crb) is necessary for apical membrane generation during gland invagination. After invagination is complete, the distal tip of the gland contacts the overlying circular visceral mesoderm (CVM) and migrates with the distal tip cells elongating and extending protrusions in the direction of migration (Bradley et al., 2003). The entire gland then turns to align itself along the anterior–posterior axis before migrating further posteriorly. In this study, we show that Rho1 GTPase regulates salivary gland invagination by maintaining apical localization of Crb, *Drosophila* atypical PKC (DaPKC) and Stardust (Sdt) and that this occurs partially through regulation of *crb* RNA level and apical localization of the transcript and by inducing apical constriction and cell shape change through Rho-kinase (Rok). The Rho–Rok signaling pathway is required again during gland migration for contraction and dorsal migration of the proximal half of the gland that allows the entire gland to turn and migrate posteriorly.

Materials and methods

Drosophila strains and Genetics

Canton-S flies were used as wild-type controls. The following fly lines were obtained from the Bloomington Stock Center and are described in FlyBase (http://flybase.bio.indiana.edu/): *Rho1*^{K02107b} (*Rho1*^{K}), *Rho1*^{1B}, *Rho1*^{72F}, *wingless* (*wg*)-GAL4, *engrailed* (*en*)-GAL4, *armadillo* (*arm*)-GAL4, UAS-*rok-CAT*, UAS-*rok-CAT-KG*, *rok*^{2}and UAS-*mouse CD8GFP* (*mCD8GFP*). UAS-*rok*RNAi was obtained from the Vienna Drosophila Research Center (VDRC). *crb*^{11A22} and UAS-*crb*^{WT} were gifts of E. Knust, UAS-*Rho1*^{N19} and UAS-*Rho1*^{V12}were gifts of N. Perrimon, UAS-*Rho1*^{WT} was a gift of N. Harden, UAS-*actinGFP*, *bagpipe* (*bap*)-GAL4 and *twist* (*twi*)-GAL4 were gifts of M. Baylies and *crb*^{11A2} *Df(3L)H99* was a gift of D. Bilder. *fork head* (*fkh*)-GAL4 was used to drive salivary gland specific expression (Henderson and Andrew, 2000).

Antibody staining of embryos

Embryos were fixed and processed for antibody staining as previously described (Reuter et al., 1990). The following antisera were used at the indicated dilutions: rat dCREB-A antiserum at 1:10,000 for DAB staining and 1:1250 for fluorescence; rabbit Fkh antiserum (a gift from M. Stern and S. Beckendorf) at 1: 1000; rabbit DaPKC antiserum (Santa Cruz Biotechnology, Inc., Santa Cruz, CA) at 1:500; mouse Crumbs antiserum (Developmental Studies Hybridoma Bank, DSHB; Iowa City, IA) at 1:100 for DAB and 1:10 for fluorescence; rabbit Stardust antiserum at 1:500 (a gift from E. Knust); mouse Neurotactin antiserum at 1:10 (DSHB); mouse α-spectrin antiserum at 1:10 (DSHB); mouse Fasciclin III (FasIII) antiserum at 1:20 (DSHB); mouse β-galactosidase (β-gal) antiserum (Promega; Madison, WI) at 1:10,000 for DAB staining and 1:500 for fluorescence; rabbit phospho-myosin light chain (p-MLC) antiserum at 1:20 (Cell Signaling Technology, Danvers, MA), rabbit Bazooka antiserum at 1:1000 (a gift from A. Brand), mouse GFP antiserum at 1:20,000 (Roche Diagnostics, Indianapolis, IN) and Alexa488-conjugated anti-GFP at 1:50 (Invitrogen Molecular Probes, OR). Appropriate biotinylated-(Jackson Immunoresearch Laboratories, Westgrove, PA), AlexaFluor488- or Rhodamine-(Molecular Probes, Eugene, OR) conjugated secondary antibodies were used at a dilution of 1:500. F-actin was labeled with AlexaFluor488-phalloidin (Molecular Probes). Whole-mount stained embryos were mounted in methyl salicylate (Sigma, St. Louis, MO), 85% glycerol with 2.5% N-propylgalate or Aqua Polymount (Polysciences, Inc., Warrington, PA). Embryos were visualized on a Zeiss Axioplan 2 microscope with Axiovision Rel 4.2 software (Carl Zeiss, Thornwood, NY) and thick (1 μm) fluorescent images were acquired on a Zeiss Axioplan microscope (Carl Zeiss) equipped for laser scanning confocal microscopy at the Rockefeller University Bio-imaging Resources Center (New York, NY).

RNA in situ hybridization

In situ hybridization with antisense digoxigenin-labeled RNA probes for *crumbs* was performed as previously described (Lehmann and Tautz, 1994). *crumbs* and *β-galactosidase* cDNAs were used as templates for generating antisense digoxygenin-labeled RNA probes as previously described (Myat and Andrew, 2002). Embryos were mounted in 70% glycerol before visualization as described above for antibody staining.

Reverse transcription (RT) and real-time PCR analyses

UAS-*Rho1*^{N19} UAS-*actinGFP*/CFL flies were crossed to *armadillo*-GAL4 flies and heterozygous and homozygous embryos were manually selected with a Zeiss Stereo Discovery V12 Zoom Microscope (Carl Zeiss). Total mRNA was extracted according to manufacturer's instructions using the QIAshredder and RNeasy mini kit from Qiagen (Valencia, CA). Reverse transcription (RT) was performed according to manufacturer's instructions using the One-Step RT-PCR kit (Qiagen). Primer sequences used for quantification of *crb* transcript were Dcrb5-3 (5′ CGCAGTCCTCTCGCCTTCTTCTAC 3′) and Dcrb3-3 (5′TGGTGCGCGAATACAGTTCCGCC 3′). Reference control was *rp49* amplified with specific primers, rp49-5-2 (5′ ATGAC-CATCCGCCCAGCATACAGG 3′) and rp49-3-2 (5′ CTCGTTCTCTTGA-GAACGCAGGCG 3′). All primers used were generated by Invitrogen (Carlsbad, CA). Intensity of the *crb* and control *rp49* PCR products was measured with NIH's ImageJ software and the ratio was calculated. Real-time PCR was performed at the Weill Cornell Microarray Core Facility.

Live imaging

Live imaging analysis was performed on the LSM 5 LIVE confocal system (Carl Zeiss) equipped with a Diode 488-100 laser. Images were acquired using either a 20X or 40X lens objective every 5 min at a scan speed between 1 and 4 for the duration of the recording period. Embryos were adhered to double-sided tape, covered in Halocarbon oil (SIGMA) and maintained at 25 °C during the recording.

Scoring of salivary gland invagination and migration phenotypes

To score gland invagination phenotypes, stage 14 embryos stained for dCREB-A were scored for glands that did not invaginate at all (None), partially invaginated with some cells that formed a tube and other cells that remained at the ventral surface (Partial) or completely invaginated (Complete). To score gland migration phenotypes, stage 14 embryos stained for dCREB-A were scored for glands that had completely turned, incompletely turned, only the distal tip turned or distal tip did not turn at all.

Quantification of fluorescence intensity and extent of apical-basal contraction

For quantification of fluorescence intensity in salivary gland placodes (Figs. 7A and D), stage 11 *en*-GAL4 UAS-*mCD8GFP* and *wg*-GAL4 UAS-*mCD8GFP* embryos were double stained for GFP and DaPKC. Three sets of Z series each consisting of three to five 0.5 μm thick optical sections were acquired by LSM confocal microscopy and the projected image of each of the Z series was analyzed by ImageJ software. Identical areas measuring 6.07 μm in width and 4.95 μm in length were selected and the ratio of the mean total signal intensity

(pixel) for GFP and DaPKC was obtained. For quantification of p-MLC fluorescence intensity in migrating salivary glands (Figs. 7I and J), stage 12 embryos were double stained for p-MLC and Fkh. Pixel intensity measurements of an area 18 μm in width and 17 μm in length were performed as described above.

For quantification of extent of apical–basal contraction, live images of *Rho1*^{1B} heterozygous and homozygous embryos at stage 11 were first acquired as described above. The distance between the apical and basal membranes of proximal gland cells at the beginning and end of the recording were measured with LSM 510 software and the average calculated. P values were obtained by STATA software two-way ANOVA analysis (StataCorp, TX).

Results

Rho1 GTPase is required for salivary gland invagination and migration

To understand how Rho1 GTPase regulates salivary gland invagination, we analyzed embryos mutant for three different alleles of Rho1, *Rho1*^{K02107b} (*Rho1*^{K}), *Rho1*^{1B} and *Rho1*^{72F} and found that gland invagination was defective in all three alleles. In *Rho1*^{K} homozygous embryos, majority of glands failed to invaginate and gland cells remained at the ventral surface of the embryo (Figs. 1D–F and J) in contrast to heterozygous embryos (Figs. 1A–C and J). Invagination defects in *Rho1*^{K} mutant glands were first observed in late stage 11. In

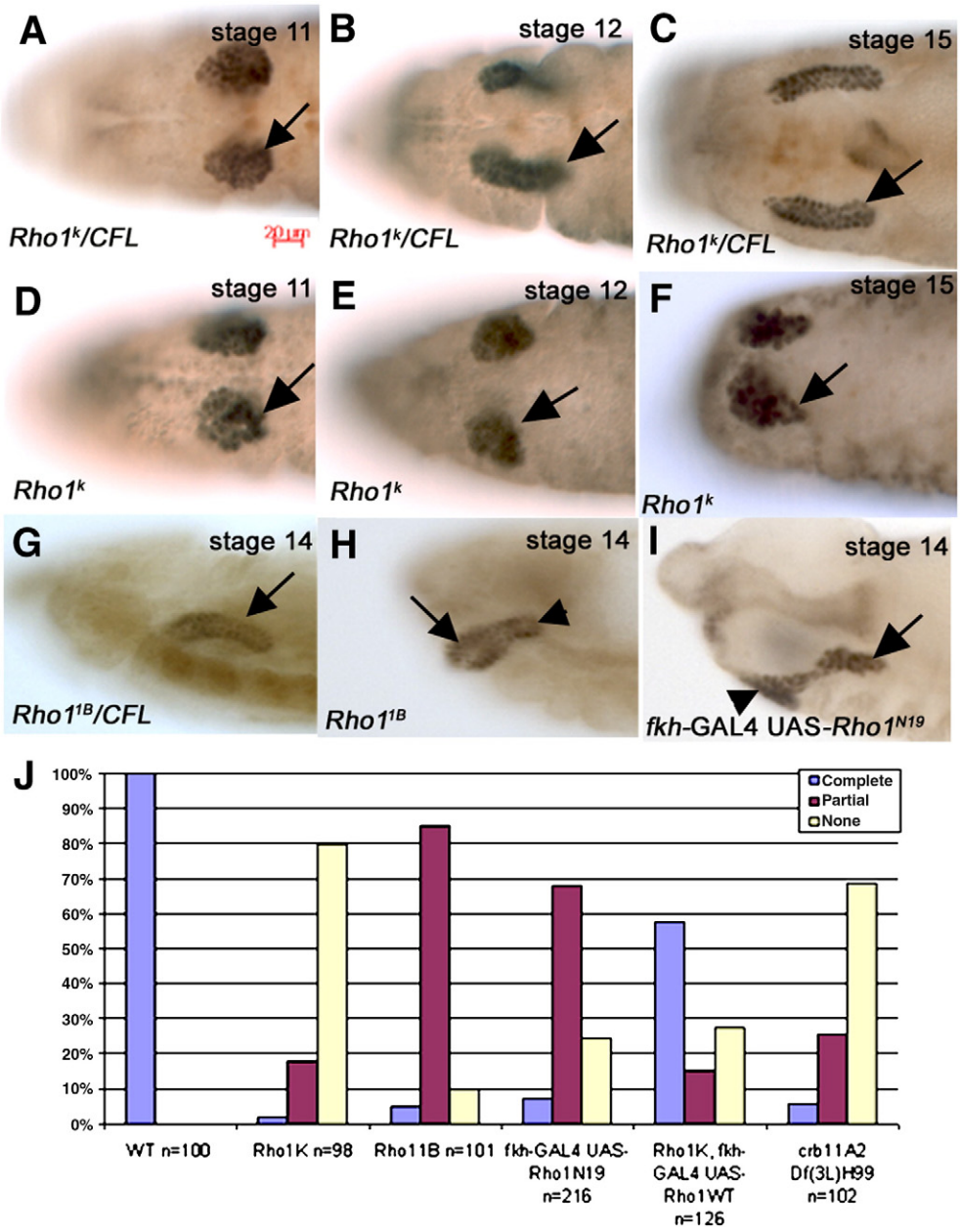

Fig. 1. Rho1 GTPase is required for salivary gland invagination and migration. *Rho1*^{K} heterozygous salivary glands invaginate (A, arrow) and migrate posteriorly (B, arrow) to form elongated glands (C, arrow). *Rho1* ^{K} homozygous glands begin to invaginate (D, arrow) but do not continue invaginating and cells remain at the ventral surface of the embryo (E and F, arrows). In embryos heterozygous for *Rho1*^{1B}, salivary glands invaginate and form elongated glands (G, arrow) whereas in *Rho1*^{1B} homozygous embryos, proximal gland cells do not invaginate (H, arrow) and the distal cells do not migrate (H, arrowhead). In embryos expressing dominant negative *Rho1*^{N19} specifically in the gland (I), some cells invaginate to form a tube (I, arrow) whereas others fail to invaginate (I, arrowhead). (J) Wild-type, mutant and recombinant embryos stained with dCREB-A were scored at stage 14 for glands that completely invaginated (Complete), partially invaginated (Partial) or did not invaginate (None). All embryos were stained for dCREB-A to mark nuclei of salivary gland cells and β-galactosidase to distinguish heterozygous from homozygous embryos.

those *Rho1*^{K} mutant glands that did invaginate, invagination always began in the correct dorsal–posterior position (data not shown). In *Rho1*^{1B} homozygous embryos, majority of glands partially invaginated (Figs. 1H and J); however, the internalized portion of the gland failed to turn and migrate posteriorly unlike heterozygous glands that turned and migrated completely (Fig. 1G). *Rho1*^{72F} homozygous embryos showed an identical phenotype to *Rho1*^{1B} homozygous embryos where majority of glands invaginated but failed to turn and migrate posteriorly (data not shown). Gland invagination and migration defects were also observed in embryos homozygous for *Df(2R)Jp1*, a deficiency that deletes the entire *Rho1* gene and *trans*-heterozygotes of *Rho1*^{K} and *Df(2R)Jp1* (data not shown). Furthermore, expression of the dominant-negative *Rho1*^{N19} mutation specifically in the gland with *fkh*-GAL4 phenocopied the *Rho1*^{K} loss of function phenotype with the majority of gland cells failing to invaginate (Figs. 1I and J).

To confirm that the gland invagination defects observed in *Rho1*^{K} mutant embryos were due to loss of Rho1 function in the gland, we expressed wild-type *Rho1* (*Rho1*^{WT}) specifically in glands of *Rho1*^{K} homozygous embryos with *fkh*-GAL4 and obtained a substantial rescue; the percentage of non-invaginated glands decreased from 80% to 27% and the percentage of completely invaginated glands increased from 2% to 58% (n=126 glands; Fig. 1J). Expression of *Rho1*^{WT} specifically in salivary glands of wild-type embryos with *fkh*-GAL4 had no effect on gland invagination (data not shown). Together, these data indicate that the invagination defects observed in *Rho1*^{K} homozygous embryos were due to lack of Rho1 function in salivary gland cells. The *Rho1*^{K} allele is due to a P-element insertion in the first intron within the coding region (Magie et al., 1999) whereas the *Rho1*^{1B} allele is an imprecise excision removing the coding region C-terminal to amino acid 52. Although no Rho protein was detected in *Rho1*^{1B} mutant embryos (Magie and Parkhurst, 2005), the phosphate binding loop and the entire effector domain that mediates binding of Rho1 to effector proteins (Self et al., 1993) are retained within the initial 52 amino acids of *Rho1*^{1B}, suggesting the possibility that this mutant protein may retain some activity. Both the *Rho1*^{K} and *Rho1*^{1B} alleles are described as strong alleles and were used in the studies described here.

Since loss of zygotic Rho1 function resulted in failure of gland cells to invaginate, we tested whether overexpression of constitutively active Rho1, *Rho1*^{V12}, in gland cells would accelerate gland invagination. In control embryos (*fkh*-GAL4+/CFL), a small group of gland cells invaginated at any given time to form elongated glands with a single lumen (Fig. S1A and B). In contrast, in *Rho1*^{V12} mutant embryos (*fkh*-GAL4 UAS-*Rho1*^{V12}) the entire placode invaginated simultaneously and cells were cuboidal shaped unlike the pyramidal shaped control cells (Fig. S1C). Continuous expression of *Rho1*^{V12}throughout gland development resulted in glands with multiple cyst-like lumena (Fig. S1D) instead of a single lumen characteristic of heterozygous glands (Fig. S1B). These data demonstrate that Rho1 activity is necessary and sufficient for gland invagination.

Rho1 activity is required for epithelial shape and apical polarity

Salivary gland cells of wild-type (Myat and Andrew, 2000a) and *Rho1*^{K} heterozygous embryos (Fig. 2A) are elongated and columnar with prominent cortical F-actin. In contrast, the salivary gland epithelium of *Rho1*^{K} homozygous embryos consisted of mesenchymal shaped cells with disorganized cortical F-actin (Fig. 2B). The loss of epithelial morphology in *Rho1*^{K} mutant embryos suggested that epithelial apical/basolateral (A/B) polarity might also be lost. In invaginating wild-type salivary glands, A/B polarity was maintained throughout the entire invagination process as indicated by the apical localization of *Drosophila* atypical Protein Kinase C (DaPKC) and Crumbs (Crb) and basolateral localization of Neurotactin (Nrt) (Fig. S2). In early salivary gland placodes of *Rho1*^{K} heterozygous and homozygous embryos, the apical protein, Crb, was localized in the apical membrane (Figs. 2C and D). However, upon initiation of invagination, apical localization of Crb was lost in the non-invaginated gland cells of *Rho1*^{K} homozygous embryos (Figs. 2F and H), whereas it was maintained in all gland cells of heterozygous embryos (Figs. 2E and G).

To test whether apical polarity in general was not maintained in *Rho1*^{K} mutant embryos or the defect was specific to Crb, we analyzed the localization of other apical proteins, DaPKC, Stardust (Sdt) and Bazooka (Baz) in *Rho1*^{K} heterozygous and homozygous embryos. DaPKC and Sdt colocalized with Crb at the apical membrane of *Rho1*^{K} heterozygous and homozygous glands prior to invagination (data not shown) but were lost from the apical membrane simultaneously with Crb at the onset of invagination in *Rho1*^{K} homozygous glands (Fig. S3). In contrast, Baz maintained its apical localization in the non-invaginated gland cells of *Rho1*^{K} homozygous embryos (Figs. 3B and B″) as in the invaginating gland cells of heterozygous embryos (Figs. 3A and A″) while Crb was lost in the homozygous gland cells (Figs. 3B and B′) and maintained in the heterozygous gland cells (Figs. 3A and A′). We next tested whether basolateral polarity was maintained or lost in *Rho1*^{K} mutant embryos by staining for the basolateral protein, Neurotactin (Nrt). Nrt maintained its normal localization at the basolateral membrane in *Rho1*^{K} homozygous gland cells as in heterozygous cells (Figs. 3C–F). Thus, these data demonstrate that zygotic activity of Rho1 is required to maintain apical polarity of a subset of apical proteins, namely, Crb, DaPKC and Sdt in invaginating gland cells and had no effect on localization of the apical protein, Baz, and the basolateral protein, Nrt.

Expression of dominant negative *Rho1*^{N19} in all cells of the salivary gland placode with *fkh*-GAL4 also led to loss of apical Crb, as in *Rho1*^{K} homozygous embryos (Fig. S4B). Furthermore, expression of *Rho1*^{N19} in only a subset of gland cells, such as the posterior two rows of the placode with *wingless* (*wg*)-GAL4, resulted in loss of apical Crb specifically in this group of cells, whereas Crb localization was normal in the remaining gland cells (Fig. S4C). Loss of Crb, DaPKC and Sdt from the apical membrane was not accompanied by mislocalization to the basolateral membrane (Figs. 2F, H and data not shown). Although Baz remained in the apical membrane of *Rho1*^{K} homozygous embryos during stages 11–14, by the end of embryogenesis the entire epidermis of *Rho1*^{K} homozygous embryos began to disintegrate and Baz was lost. This is consistent with previous reports that DE-cad, as well as β-catenin and α-catenin were disrupted in the epidermis of Rho mutant embryos at stage 15 (Magie et al., 2002).

In *Drosophila*, *crb* is required for maintenance of epithelial polarity and proper positioning of adherens junctions (Grawe et al., 1996; Izaddoost et al., 2002; Klebes and Knust, 2000; Pelllkka et al., 2002). In embryos homozygous for *crb*^{11A22}, salivary gland cells die (Fig. S5A and B) and small glands are formed due to degeneration of the epithelium as previously described (Grawe et al., 1996; Tepass and Knust, 1990; Tepass and Knust, 1993). Therefore, we analyzed embryos homozygous for *crb*^{11A2} and *Df(3L)H99* (*crb*^{11A2} *Df(3L)H99*) that fail to undergo apoptosis due to the *H99* deletion (Bilder et al., 2003). In *crb*^{11A2} *Df(3L)H99* homozygous embryos, 68.7% of glands failed to invaginate, 25.6% partially invaginated and 5.7% completely invaginated (n=102 glands; Figs. 1J and S5D). Salivary gland invagination defects in *crb*^{11A2} *Df(3L)H99* mutant glands were accompanied by loss of A/B polarity. In the early gland epithelium of *crb*^{11A2} *Df(3L)H99* heterozygous embryos, DaPKC was localized apically and Nrt was localized basolaterally (Fig. S5E) whereas in homozygous embryos, neither DaPKC nor Nrt showed a polarized localization and instead was diffused in the cytoplasm (Fig. S5F). These data demonstrate that proper polarization of salivary gland cells is required for invagination and that Rho1 GTPase plays an important role in maintaining apical polarity during invagination.

We previously showed that *crb* RNA becomes elevated in the apical domains of salivary gland cells prior to and during invagination in a manner partially dependent on the transcription factor,

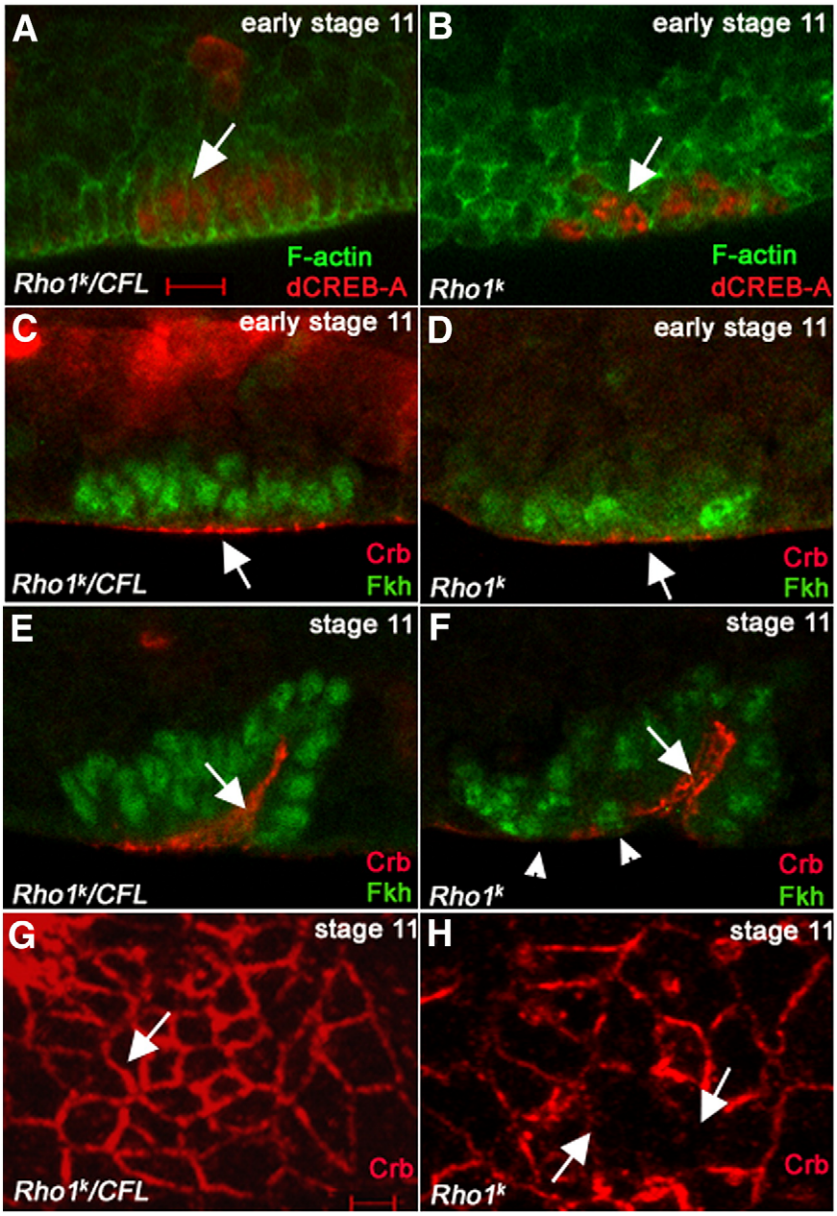

Fig. 2. Rho1 activity is required for epithelial shape and Crb localization. Salivary gland cells of $Rho1^{K}$ heterozygous embryos are columnar with prominent F-actin (A, arrow) whereas cells of $Rho1^{K}$ homozygous embryos are mesenchymal-shaped with disorganized F-actin (B, arrow). In $Rho1^{K}$ heterozygous embryos (C), Crb (red) in salivary gland cells marked by Fkh (green) is localized in the apical membrane before (C, arrow) and during invagination (E, arrow). In $Rho1^{K}$ homozygous embryos (D and F), Crb (red) is localized in the apical membrane of gland cells before invagination (D, arrow) and in the internalized cells (F, arrow) during invagination but is lost in the gland cells that do not invaginate (F, arrowheads). Projected images of ten 1 μm Z optical sections of $Rho1^{K}$ heterozygous (G) and homozygous glands (H) show that Crb is lost in the homozygous glands (H, arrows) unlike in heterozygous glands (G, arrow). Embryos in panels A and B were stained for phalloidin to label F-actin (green) and dCREB-A (red) to mark salivary gland nuclei, embryos in panels C–H were stained for Crb (red) to mark the apical membrane and embryos in panels C–F were also stained for Fkh (green) to mark gland nuclei. All embryos were stained for β-gal to distinguish heterozygous from homozygous embryos. All panels shown are lateral views of embryos except for the embryos in G and H which are horizontal views. Scale bar in panel A represents 10 μm and scale bar in panel G represents 2 μm.

Huckebein (Myat and Andrew, 2002). Moreover, it was recently reported that in *Drosophila* follicular cells, dynein transports Crb protein and RNA to the apical membrane (Li et al., 2008). To test whether the loss of Crb protein observed in $Rho1^{K}$ homozygous embryos is in part due to reduced *crb* transcript levels and/or apical localization, we performed real time and RT-PCR analyses of wild-type embryos expressing dominant negative $Rho1^{N19}$ in the entire epidermis with *arm*-GAL4 and whole mount in situ hybridization (ISH) of *crb* RNA in $Rho1^{K}$ mutant embryos. We observed a 10% decrease in *crb* RNA levels in $Rho1^{N19}$ mutant embryos by real-time PCR and RT-PCR compared to control embryos suggesting that the loss of Crb protein observed in $Rho1^{K}$ mutant embryos is in part due to reduced *crb* transcription. In non-invaginating gland cells of $Rho1^{K}$ heterozygous embryos, *crb* RNA was elevated compared to surrounding non-gland cells, consistent with our previous findings (Fig. 4A) (Myat and Andrew, 2002). In contrast, in non-invaginating gland cells of $Rho1^{K}$ homozygous embryos with a similar apical domain size, *crb* RNA was not elevated in the apical domains of gland cells (Fig. 4B) or elsewhere in the cells. We observed a similar reduction of apical *crb* RNA specifically in gland cells expressing dominant negative $Rho1^{N19}$ (Fig. 4D) compared to control gland cells (Fig. 4C). Thus, these data demonstrate that the loss of Crb protein due to absence of zygotic Rho1 activity is in part due to reduced *crb* RNA levels and apical localization of the transcript.

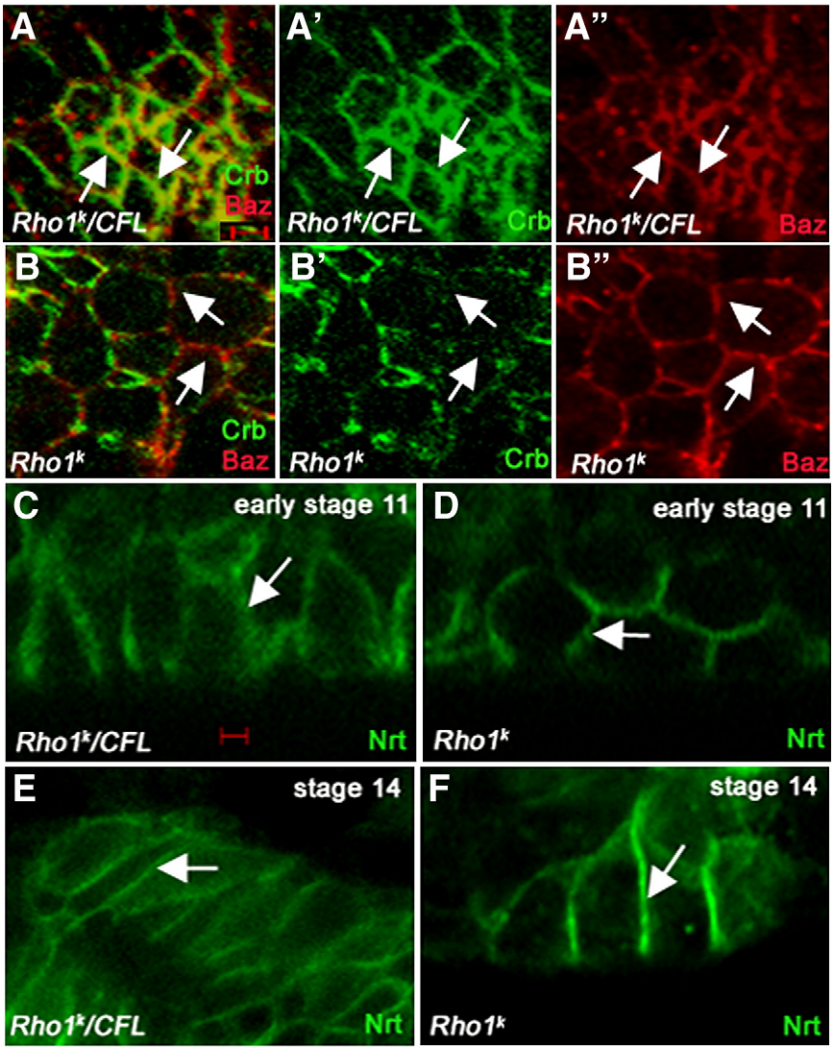

Fig. 3. Baz and Nrt are maintained in invaginating Rho1 mutant glands. In $Rho1^K$ heterozygous (A) and homozygous (B) embryos, Baz (A, A″, B and B″, red) is localized at the apical membrane of invaginating heterozygous gland cells (A and A″, arrows) and noninvaginating homozygous gland cells (B and B″, arrows) whereas Crb (A, A′, B and B′, green) is maintained in heterozygous gland cells (A and A′, arrows) and is lost in homozygous gland cells (B and B′, arrows). In $Rho1^K$ heterozygous (C and E) and homozygous (D and F) embryos, Nrt is localized in the basolateral membrane of gland cells at stages 11 (C and D, arrows) and 14 (E and F, arrows). Embryos in panels A and B were stained for Crb (green) and Baz (red) and embryos in panels C–F were stained for Nrt (green) to mark the basolateral membrane. Heterozygous and homozygous embryos were distinguished by β-gal staining on the CFL balancer chromosome (not shown). Panels in A and B are horizontal views of gland cells whereas panels in panels C–F are lateral views of embryos. Scale bar in panel A represents 2 μm and scale bar in panel C represents 1 μm.

Rho1 regulates gland invagination through Crb and Rok

Since Rho1 activity regulated *crb* transcript levels, we tested whether expression of wild-type *crb* (crb^{WT}) in $Rho1^K$ mutant glands through a heterologous promoter will rescue the polarity and/or invagination defects. In the early gland placode of $Rho1^K$ heterozygous embryos (Fig. 4E) and wild-type embryos expressing crb^{WT} specifically in the gland (Fig. 4F), Crb was localized in the apical membrane, albeit Crb was more robust in the latter embryos. Crb was lost in gland cells of $Rho1^K$ homozygous embryos (Fig. 4G); however, Crb was restored to the apical membrane of $Rho1^K$ homozygous embryos expressing crb^{WT} specifically in gland cells (Fig. 4H). Restoration of apical Crb in $Rho1^K$ homozygous embryos expressing crb^{WT} also restored apical DaPKC (Fig. 4K) and Sdt (data not shown). In stage 14 wild-type glands (Fig. 4I), DaPKC was localized at the apical membrane and Nrt at the basolateral membrane. In stage 14 wild-type glands expressing crb^{WT}, DaPKC was localized around the entire plasma membrane and Nrt was lost (Fig. 4J), demonstrating the expansion of the apical membrane at the expanse of the baslateral membrane due to ectopic Crb. Even at stage 14, DaPKC in $Rho1^K$ homozygous glands expressing crb^{WT} remained at the apical domain in most gland cells and in other cells was distributed around the entire plasma membrane (Fig. 4K). These data show that Crb is necessary and sufficient to maintain apical polarity of DaPKC and Sdt in the gland epithelium downstream of Rho1 activity. Overexpression of crb^{WT} in $Rho1^K$ homozygous embryos also rescued the gland invagination defect to a small extent; the number of non-invaginated glands decreased from 80% in $Rho1^K$ homozygous embryos to 68% (n=120 glands) with a concomitant increase in the number of partially invaginated glands from 18% to 29% (Fig. 5I).

In crb^{WT} expressing $Rho1^K$mutant glands that failed to invaginate, apical domains did not constrict even though apical localization of Crb and DaPKC was restored (Figs. 4H and K), suggesting that additional processes downstream of Rho1 were required to achieve apical constriction and invagination. To test this hypothesis, we determined whether Rho-kinase (Rok), a known regulator of apical constriction in *Drosophila* epithelia (Dawes-Hoang et al., 2005), mediated apical constriction downstream of Rho1 during gland invagination. In a small percentage of embryos mutant for rok^2, a strong loss-of-function allele of *rok* (Winter et al., 2001), glands failed to invaginate or did not invaginate completely (9%, n=170 glands) and often began with anterior gland cells (Fig. 5A) instead of dorsal–posterior cells, as

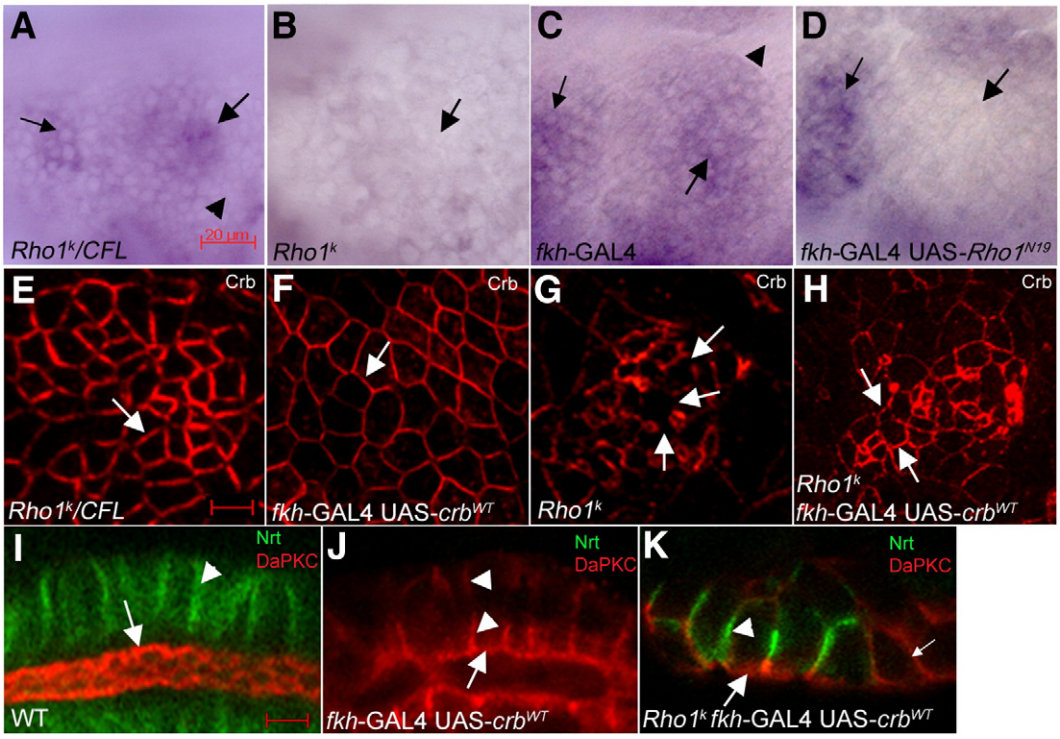

Fig. 4. Rho1 maintains apical polarity through *crb*. In $Rho1^K$ heterozygous (A) and *fkh*-GAL4 control (C) embryos, *crb* RNA is elevated in the apical domains of salivary gland cells (A and C, large arrows) compared to neighboring non-gland cells (A and C, arrowheads). In $Rho1^K$ homozygous embryos (B) and wild-type embryos overexpressing dominant negative $Rho1^{N19}$ specifically in the gland (D), *crb* RNA is lost from the apical domain of gland cells (B and D, large arrows). In the early gland placode of $Rho1^K$ heterozygous embryos (E) and wild-type embryos overexpressing crb^{WT} in the gland (F), Crb is localized at the apical membrane (E and F, arrows). Crb is lost in $Rho1^K$ mutant glands (G, arrows), whereas it is maintained in $Rho1^K$ mutant glands overexpressing crb^{WT}(H, arrows). In stage 14 wild-type glands (I), DaPKC is localized at the apical membrane (I, arrow) and Nrt at the basolateral membrane (I, arrowhead). In stage 14 wild-type glands overexpressing crb^{WT} (J), DaPKC is localized at the apical membrane (J, arrow) and in more basal regions (J, arrowheads), whereas Nrt is completely lost. In stage 14 glands of $Rho1^K$ homozygous embryos overexpressing crb^{WT} (K), DaPKC (K, large arrow) is localized exclusively at the apical membrane and Nrt (K, arrowhead) at the basolateral membrane in most cells but in some cells DaPKC is localized around the entire plasma membrane (K, small arrow) and Nrt is lost. All panels shown are horizontal views except for panels I, J and K which are lateral views. Embryos in panels A–H are at stage 11, whereas embryos in panels I, J and K are at stage 14. In panels A–D, cells anterior to the salivary gland (A, C and D, small arrows) express high levels of *crb* RNA and serve as an internal control for ISH. Gland cells in panels A–D were identified by the position of the gland placode in parasegment 2 and gland cells in panels E–H were identified by double staining for dCREB-A (not shown). Scale bars in panels E and I represent 5 μm.

in wild-type embryos. rok^2mutant embryos also showed gland migration defects (35%, $n=170$ glands) where the distal tip cells turned but the proximal half of the gland did not turn and the gland failed to migrate posteriorly (Fig. 5B). Gland invagination and migration defects were also observed in glands where *rok* was inhibited in the entire epidermis with RNAi (Fig. 5C, D and Fig. S6). In rok^2 mutant glands, apical localization of Crb was not lost (Fig. 5F) in contrast to $Rho1^K$ mutant glands. However, apical constriction was defective in rok^2 mutant glands (Fig. 5H) in contrast to heterozygous glands that constricted apically and invaginated (Fig. 5G). The low penetrance of gland invagination defects in rok^2 homozygous embryos is likely due to the significant maternal contribution of *rok* (Mizuno et al., 1999). In support of this, a slight increase in gland invagination defects was observed when *rok* function was inhibited with RNAi (13%, $n=159$ glands) compared to rok^2 homozygous embryos lacking zygotic function of *rok* (9%, $n=170$ glands). Although invagination site was changed from dorsal–posterior to anterior section of the salivary gland placode in rok^2 homozygous embryos, in glands where *rok* was knocked down with RNAi, invagination began in the correct dorsal–posterior position (data not shown). These data demonstrate that Rok is not required for apical localization of Crb and is instead required for apical constriction and cell shape change during gland invagination.

To determine whether Rok functions downstream of Rho1 to mediate gland invagination we tested the ability of the catalytic domain of *rok*, *rok-CAT*, known to confer increased rok activity independent of Rho (Winter et al., 2001), to rescue the gland invagination defect of $Rho1^K$ homozygous embryos. Overexpression of *rok-CAT* in wild-type glands had no effect on invagination and migration but resulted in expansion of the gland lumen in late embryogenesis (Fig. S1E and F). Expression of *rok-CAT* specifically in salivary glands of $Rho1^K$ mutant embryos led to a partial rescue of the gland invagination defect; the percentage of non-invaginated glands decreased and the percentage of partially and completely invaginated glands increased compared to $Rho1^K$ mutants (Fig. 5I). Since crb^{WT} and *rok-CAT* each partially rescued the gland invagination defect of $Rho1^K$ mutant embryos, we next tested whether simultaneous expression of crb^{WT} and *rok-CAT* in salivary glands of $Rho1^K$ homozygous embryos would result in a better rescue of the $Rho1^K$ invagination defect. Coexpression of crb^{WT} and *rok-CAT* indeed led to a better rescue of the gland invagination defect of $Rho1^K$ homozygous embryos compared to expression of either transgene alone (Fig. 5I). In contrast, coexpression of *rok-CAT-KG*, encoding a kinase dead form of Rok (Winter et al., 2001) and crb^{WT} in $Rho1^K$ homozygous embryos did not increase the level of rescue observed with crb^{WT} alone (Fig. 5I). One functional output of the Rho–Rok signaling pathway is the increased phosphorylation of myosin resulting in actin–myosin contraction. Therefore, we tested whether Rho and Rok regulated gland invagination through phoshorylation of myosin light chain. In $Rho1^K$ heterozygous embryos, phosphorylated myosin-light-chain (p-MLC) accumulated in the apical membrane prior to and during gland invagination (Figs. S7A and B). In contrast, p-MLC was reduced in the non-invaginated glands of $Rho1^K$ homozygous embryos (Fig. S7C and D). These data demonstrate that Rho1 GTPase controls gland invagination through both Crb and Rok to maintain polarity of a subset of apical proteins and to activate actin-myosin contraction, respectively.

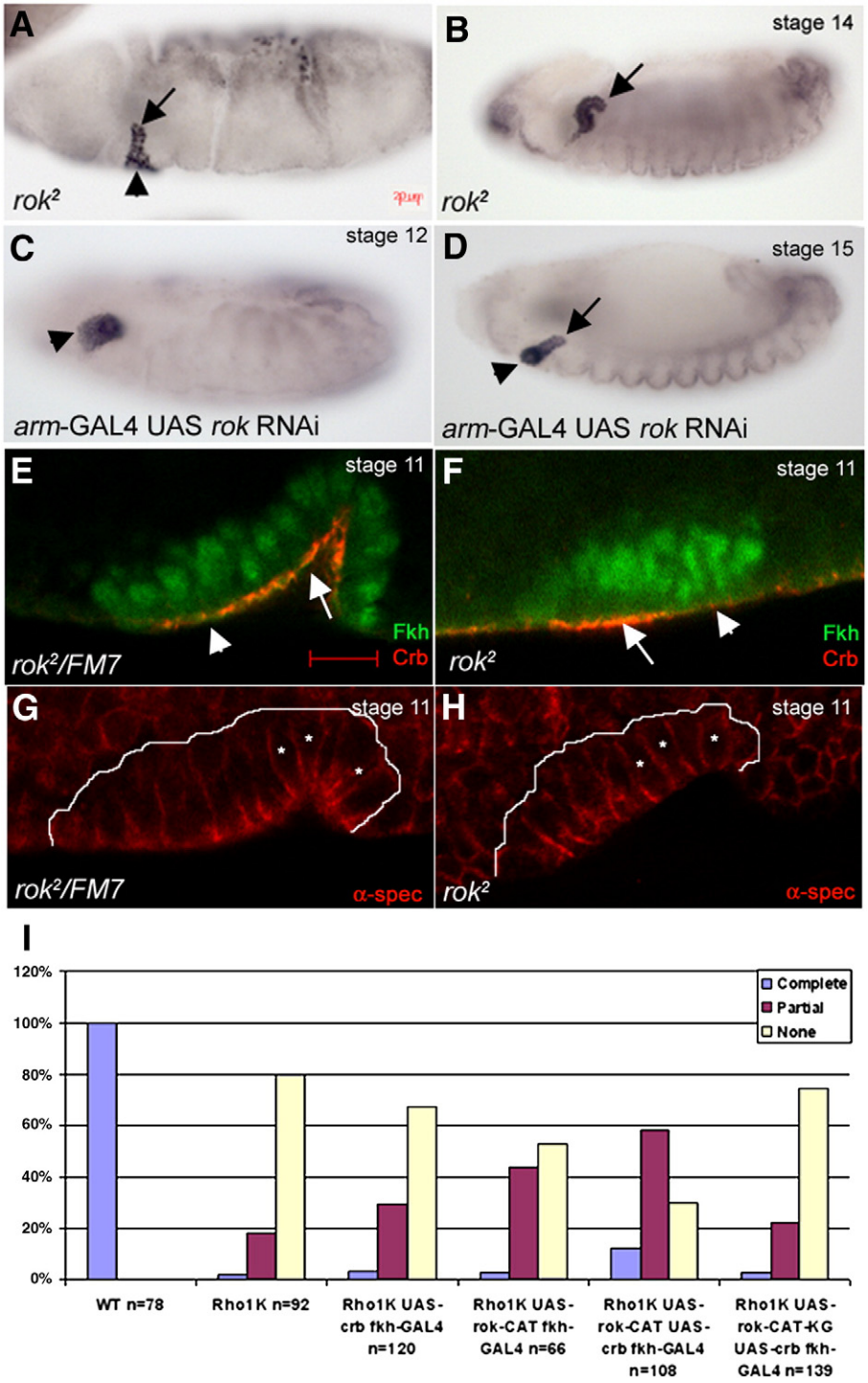

Fig. 5. Rok and Crb control salivary gland invagination downstream of Rho1. In rok^2 mutant embryos (A and B), glands invaginate partially (A, arrow) with some cells remaining at the embryo surface (A, arrowhead) or invaginate completely but fail to turn and migrate posteriorly (B, arrow). In embryos where *rok* RNAi is expressed in the entire epidermis with *arm*-GAL4 (C and D), glands do not invaginate (C and D, arrowheads) or do not migrate (D, arrow). In rok^2 heterozygous embryos (E), Crb is localized apically in the invaginating dorsal–posterior gland cells (E, arrow) and in the non-invaginating cells (E, arrowhead), whereas in rok^2 homozygous embryos (F), Crb is localized apically in the invaginating anterior gland cells (F, arrow) and in the non-invaginating cells (F, arrowhead). rok^2 heterozygous gland cells constrict apically and invaginate (G, asterisks), whereas homozygous gland cells do not constrict apically (H, asterisks). Graph (I) depicts extent of gland invagination phenotypes in wild-type embryos, $Rho1^K$ homozygous embryos, $Rho1^K$ homozygous embryos expressing crb^{WT} or *rok-CAT* and $Rho1^K$ homozygous embryos coexpressing crb^{WT} and *rok-CAT* or crb^{WT} and *rok-CAT-KG*. Embryos in panels A–D were stained for DCREB-A. Embryos in panels G and H were stained for α-spectrin (α-spec) to label cell outlines and Fkh (not shown). White lines in panels G and H mark the outline of the gland which is based on Fkh staining (not shown). Scale bar in panel E represents 10 μm.

Rho1 mediates cell contraction during salivary gland migration

Our genetic analysis of *Rho1* and *rok* mutants demonstrated that Rho–Rok signaling was required not only for gland invagination but also for migration (Figs. 5A–D and Fig. S6). Since Rok is an important regulator of actin–myosin contraction we sought to determine whether cell contraction plays a role in gland migration. We analyzed normal gland migration by live-imaging wild-type glands expressing either mouse CD8GFP in the entire gland with *fkh*-GAL4 (Fig. 6A and Movie 1) or actinGFP in a cluster of proximal gland cells with *en*-GAL4

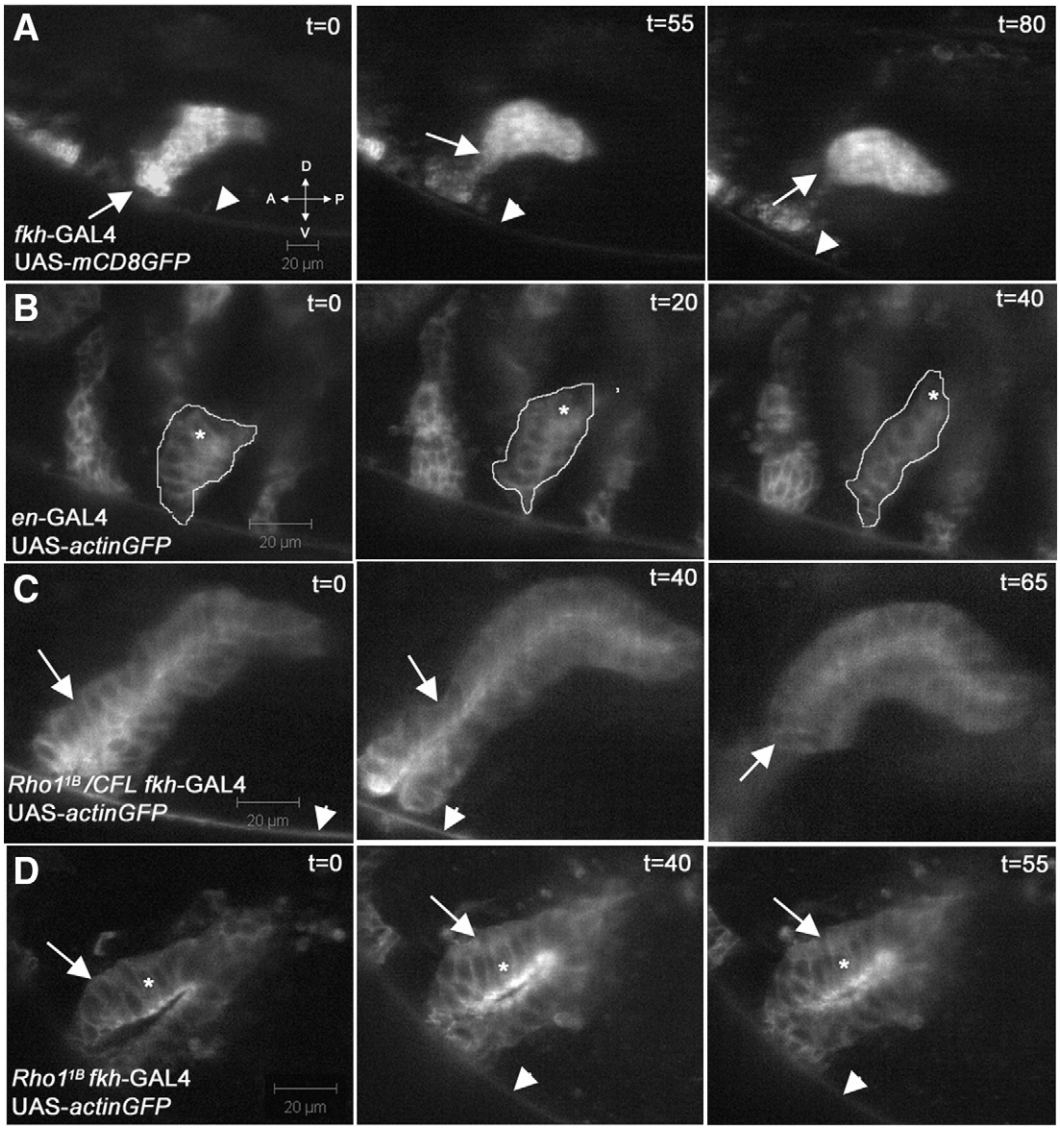

Fig. 6. Rho1-dependent cell contraction is required for gland migration. Live-imaging of wild-type salivary gland expressing mCD8GFP in the entire gland with *fkh*-GAL4 (A) shows the proximal tip of the gland (A, arrows) contract and migrate away from the embryo surface (A, arrowheads) followed by posterior turning of the entire gland. Live-imaging of wild-type salivary gland expressing actinGFP in a cluster of proximal gland cells with *en*-GAL4 (B) shows apical–basal contraction, rounding and dorsal migration. Live-imaging of $Rho1^{1B}$ heterozygous (C) and homozygous (D) glands expressing actinGFP in all gland cells with *fkh*-GAL4 shows that $Rho1^{1B}$ heterozygous gland cells in the proximal half of the gland contract (C, arrows) resulting in detachment of the proximal gland from the embryo surface (C, arrowheads) whereas $Rho1^{1B}$ homozygous gland cells do not contract (D, arrows) and the gland remains close to the embryo surface (D, arrowheads) and fails to migrate posteriorly. Asterisks in panels B and D mark the movement of a single cell during the recording period. Recording time (t) is shown in minutes. White line in the B panels outlines proximal gland cells. D: dorsal, V: ventral, A: anterior and P: posterior.

(Fig. 6B and Movie 2) and $Rho1^{1B}$ heterozygous glands expressing actinGFP with *fkh*-GAL4 (Fig. 6C and Movie 3) at the stage when all gland cells had invaginated but the gland had not migrated yet. In wild-type glands, columnar cells in the proximal half of the gland contracted coordinately in the apical–basal axis to become round and moved dorsally away from the ventral surface of the embryo (Figs. 6A–C, Movies 1, 2 and 3). In contrast, $Rho1^{1B}$ mutant gland cells did not contract in the apical–basal axis and did not migrate dorsally (Fig. 6D and Movie 4). We quantified the $Rho1^{1B}$ cell contraction defect by measuring the distance between the apical and basal membranes of $Rho1^{1B}$ heterozygous and homozygous proximal gland cells labeled with actinGFP (see Materials and Methods). During the 50 min of live recording, $Rho1^{1B}$ heterozygous cells in the proximal half of the gland contracted from 12.5 μm to 8.6 μm in length ($n=18$ cells, $p=0.0000$). In contrast, $Rho1^{1B}$ homozygous gland cells showed no contraction and measured 16 μm at the beginning and end of the recording ($n=12$ cells, $p=0.7249$). Thus, our live-imaging studies provide the first evidence for coordinated cell contraction and a rounded type of motility in the proximal half of the gland during migration and the identification of Rho1 GTPase as a key regulator of this process.

To confirm that the $Rho1^{1B}$ gland migration defect was due to absence of Rho1 activity in gland cells, we attempted to rescue the $Rho1^{1B}$ migration defect by expressing wild-type Rho1 ($Rho1^{WT}$) in all gland cells. Expression of $Rho1^{WT}$ in all $Rho1^{1B}$ mutant gland cells with *fkh*-GAL4 resulted in a partial rescue of the gland migration defects; percentage of glands that turned incompletely and completely increased in the rescue embryos with an accompanying decrease in the percentage of glands that did not turn at all and only the tip turned (Fig. 7G). Since our data showed contractile motility of the proximal gland cells which contrasted from the previously described elongated motility of distal tip cells (Bradley et al., 2003), we next tested whether Rho1 activity was required for both types of movement. We used the *en*-GAL4 and the *wg*-GAL4 lines to achieve transgene expression in a cluster of proximal gland cells or distal gland cells, respectively (Figs. 7A–F). Initial studies with mouse CD8GFP driven by either *en*-Gal4 or *wg*-GAL4 confirmed that *en*-GAL4 drove expression robustly in a

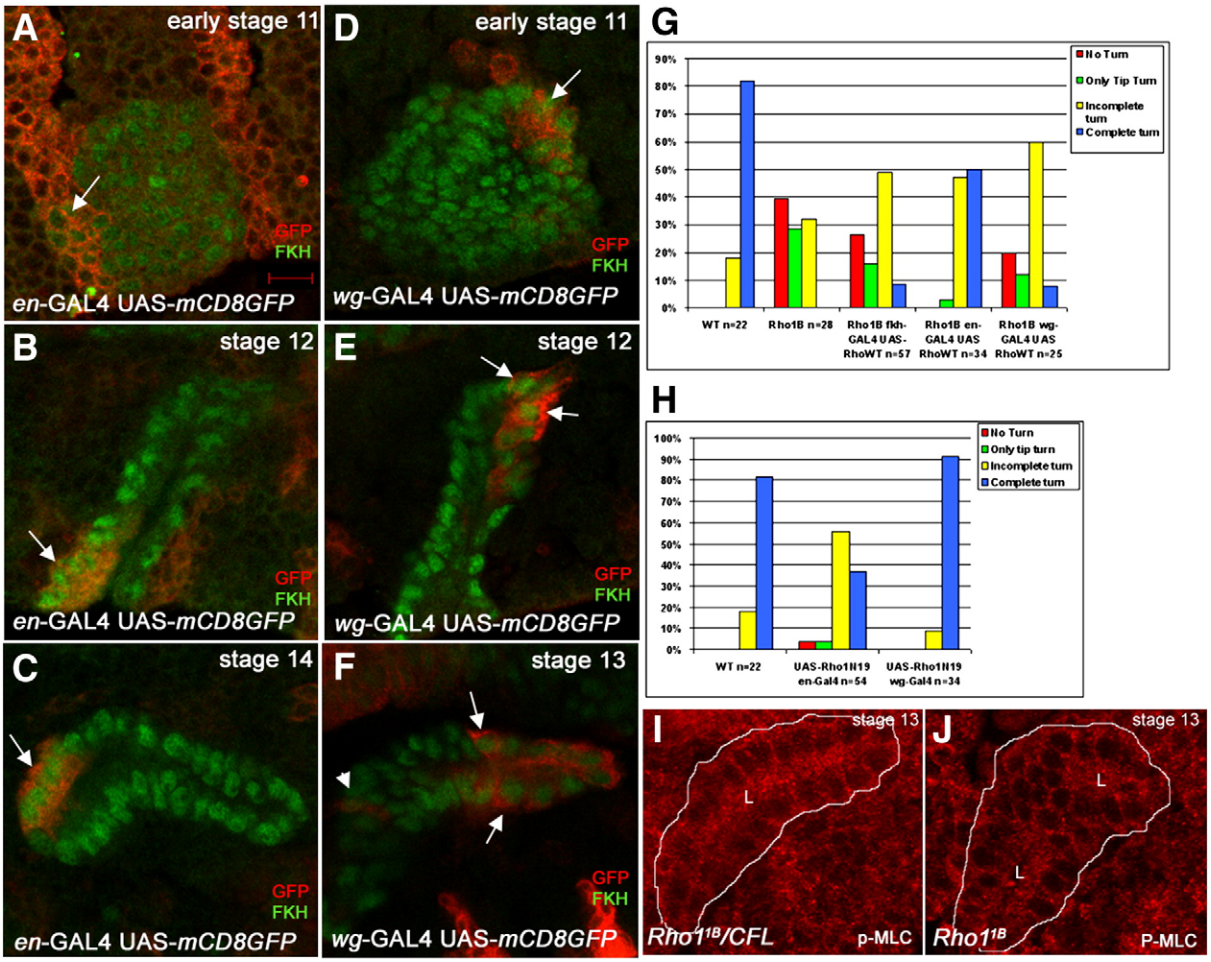

Fig. 7. Rho1 function is required predominantly in the proximal gland cells for migration. In wild-type embryos where mCD8GFP expression is driven by *en*-GAL4 (A–C), GFP (A–C, red) is expressed in the anterior-most cluster of placode cells prior to gland invagination (A, arrow), in a cluster of proximal gland cells (B, arrow) as the gland begins to migrate and continues to be expressed in the proximal gland cells (C, arrow) during later stages of migration. In wild-type embryos where mCD8GFP expression is driven by *wg*-GAL4 (D–F), GFP (D–F, red) is expressed in the dorsal–posterior cells during gland invagination (D, arrow). *wg*-GAL4 driven mCD8GFP is later expressed in the distal cells including the elongated distal tip cells (E, arrows) as the gland begins to migrate and in the distal-half of the gland (F, arrows) during later stages of migration. A single *wg*-GAL4 UAS-mCD8GFP gland cell is occasionally observed in a more proximal location (F, arrowhead). (G) Graph depicts extent of gland migration in stage 14 wild-type embryos, $Rho1^{1B}$ homozygous embryos and $Rho1^{1B}$ homozygous embryos where $Rho1^{WT}$ was expressed in all gland cells with *fkh*-GAL4, proximal gland cells with *en*-GAL4 or distal gland cells with *wg*-GAL4. (H) Graph depicts extent of gland migration in stage 14 wild-type embryos and wild-type embryos expressing $Rho1^{N19}$ in proximal gland cells with *en*-GAL4 or in distal gland cells with *wg*-GAL4. In migrating glands of $Rho1^{1B}$heterozygous embryos (I), phosphorylated MLC (p-MLC) is prominent in all cells (I) whereas in cells of $Rho1^{1B}$homozygous glands, p-MLC is decreased (J). Embryos in panels A–F were stained for GFP (red) and Fkh (green) to label gland cells. Embryos in panels I and J were stained for p-MLC (red) and dCREB-A (not shown). White lines in panels I and J outline the gland. Salivary gland lumen in panels I and J is marked by L. Scale bar in panel A represents 10 μm.

cluster of proximal gland cells (Figs. 7A–C and S8A) and to a lesser extent in clusters of CVM cells (Fig. S8A) whereas *wg*-GAL4 drove expression robustly in the distal gland cells (Figs. 7D–F and S8B) and to a lesser extent in the entire CVM (Fig. S8B). Interestingly, rescue of the $Rho1^{1B}$ migration defect with *en*-GAL4 driven expression of $Rho1^{WT}$ led to a significantly better rescue than with *wg*-GAL4 (Fig. 7G) suggesting a greater requirement for Rho1 activity in the proximal gland cells than in the distal cells. *en*-GAL4 driven expression of $Rho1^{WT}$ also led to a better rescue than with *fkh*-GAL4 which could be due to the earlier embryonic expression of $Rho1^{WT}$ by *en*-GAL4 compared to *fkh*-GAL4. Alternatively, spatial regulation of Rho1 activity may be important for gland migration and uniform overexpression of $Rho1^{WT}$ in the entire gland with *fkh*-GAL4 may have inhibitory effects on gland migration. To test this possibility, we expressed $Rho1^{WT}$ in the entire gland with *fkh*-GAL4 of otherwise wild-type embryos and analyzed gland migration at different stages of embryogenesis. Gland migration was delayed at stage 12 in glands overexpressing $Rho1^{WT}$; however, this delay in gland migration was corrected by stage 14 (Fig. S9). Thus, spatial expression of Rho1 within the gland appears to be important for efficient gland migration.

Expression of dominant negative $Rho1^{N19}$ in the proximal gland cells with *en*-GAL4 or in the distal gland cells with *wg*-GAL4 also showed that inhibition of Rho1 function in the proximal cells was more deleterious for gland migration than inhibition in the distal cells (Fig. 7H). We confirmed that *en*-GAL4 and *wg*-GAL4 mediated transgene expression at similar levels by embryonic stage 11 when the salivary gland placodes form by measuring the levels of GFP fluorescent intensity of gland cells expressing *en*-GAL4 driven or *wg*-GAL4 driven mCD8GFP (data not shown). Therefore, these studies show that normal Rho1 activity is more critical in the proximal cells than in the distal cells of the migrating gland and that Rho1-dependent contraction and dorsal migration of proximal cells is a key element of turning and migration of the entire gland.

To test whether Rho1 controlled proximal gland cell contraction and migration through activation of actin-myosin contraction, we stained $Rho1^{1B}$ mutant embryos for p-MLC. In $Rho1^{1B}$ heterozygous embryos, prominent p-MLC staining was found throughout the cells of migrating glands (Fig. 7I) whereas glands of $Rho1^{1B}$ homozygous embryos showed decreased p-MLC staining (Fig. 7J). We quantified the level of p-MLC in glands of $Rho1^{1B}$ heterozygous and homozygous embryos and found

that p-MLC fluorescence intensity in *Rho1*^{1B} mutant glands was reduced to 78% of the intensity of heterozygous glands. These data suggest that Rho1 regulates gland migration in part through phosphorylation of MLC and subsequent actin-myosin contraction.

Rho1 function is required in both the salivary gland and CVM for gland migration

Expression of *Rho1*^{WT} in all or a subset of salivary gland cells of *Rho1*^{1B} mutant embryos did not completely rescue the gland migration defects (Fig. 7G). Furthermore, *en*-GAL4 and *wg*-GAL4 drove transgene expression in the CVM in addition to the gland (Fig. S8A and B). These data raised the possibility that Rho1 might regulate gland migration in a cell non-autonomous manner. Thus, we tested whether Rho1 activity is also required in the circular visceral mesoderm (CVM) upon which the gland migrates. The CVM is derived from the trunk visceral mesoderm primordia which ingresses into the interior of the embryo to form cell clusters that then expand along the anterior-posterior (A-P) axis to form a continuous layer (Fig. S10A and B) (Lee et al., 2005). In *Rho1*^{1B} homozygous embryos, the CVM was discontinuous with clusters of cells at discrete intervals along the A-P axis (Fig. S10C and D). Furthermore, expression of dominant negative *Rho1*^{N19} in the CVM with *twist* (*twi*)-GAL4 that drives transgene expression in the CVM and somatic mesoderm (SM) (Fig. S8C) resulted in failure of the glands to turn and migrate posteriorly (Fig. S10F). These gland migration defects correlated with failure to form a properly structured CVM where the cells were spindle shaped and did not elongate in the dorsal–ventral axis (Fig. S10F), as in control embryos (Fig. S10E). Due to these CVM defects observed upon loss of *Rho1* function, we next tested whether expression of *Rho1*^{WT} in the mesoderm could rescue the gland migration defects of *Rho1*^{1B} homozygous embryos. Expression of *Rho1*^{WT} in the entire CVM of *Rho1*^{1B} homozygous embryos with *twi*-GAL4 (Fig. S8C) partially rescued the gland migration defect albeit to a weaker extent than with *en*-GAL4 (compare Fig. S10G to Fig. 7G). Similar level of rescue was observed when *Rho1*^{WT} was expressed in clusters of the CVM of *Rho1*^{1B} homozygous embryos with *bap*-GAL4 (Figs. S8D and S10G). These data demonstrate that Rho1 activity is required for proper development of the CVM; however, Rho1 activity is required predominantly in the proximal gland cells for their contraction and migration.

Discussion

In this study, we demonstrate that Rho1 activity controls salivary gland invagination through at least two distinct mechanisms; one, by maintaining apical polarity specifically of Crb, DaPKC and Sdt in the early salivary gland placode and two, by inducing apical constriction and cell shape change through Rok in the invaginating gland (Fig. 8A). Since simultaneous expression of Crb and Rok did not result in complete rescue of the Rho invagination defect, it is possible that Rho regulates gland invagination by other as yet unidentified mechanism (s) in addition to Crb and Rok. We show that Rho1 and Rok are required again during gland migration to control cell contraction and rounded movement of the proximal half of the gland (Figs. 8A and B). Our live-imaging and genetic analyses provide the first evidence that cell contraction and rounded motility of cells in the proximal half of the gland is essential for turning and subsequent posterior migration of the entire gland. Although Rho1 activity is required in the gland cells and in the CVM for gland migration, Rho1 activity is required predominantly in the proximal gland cells for contraction and migration.

We show that zygotic function of Rho1 is required to prevent loss of the apical proteins, Crb, DaPKC and Sdt in the invaginating salivary gland and not of the apical protein, Baz, demonstrating that Rho1 activity regulates a specific subset of apical proteins and not apical polarity in general. Rho1 activity maintains Crb protein in salivary gland cells in part by regulating *crb* RNA levels and apical localization of the transcript. Since Rho GTPases are important regulators of the actin and microtubule cytoskeletal systems which together with their respective motor proteins, are required for the proper delivery of mRNA to one membrane domain or the other of polarized cells (St Johnston, 2005), it is possible that *crb* transcripts fail to localize in the apical domain of Rho1 mutant cells because they are not transported to and/or stabilized at the apical membrane due to underlying defects in the apical cytoskeleton. Rho GTPases have been shown to regulate RNA stability such as those of the Na^+/Ca^{2+}exchanger (Maeda et al., 2005) and endothelial nitric oxide synthase mRNAs (Laufs and Liao, 1998) although the mechanism is unknown.

Although loss of Crb, DaPKC and Sdt occurred simultaneously in Rho1 mutant glands, overexpression of *crb*^{WT} from a heterologous promoter was sufficient to restore expression and apical localization not only of Crb but also of Sdt and DaPKC. These data suggest that apical Crb maintains DaPKC and Sdt in their proper localization at the apical membrane either directly or through Crb-mediated stabilization of the sub-membrane cytoskeleton. A recent study reported that the Dynein motor localizes Crb in follicle cells through apical targeting of *sdt* RNA (Horne-Badovinac and Bilder, 2008). Therefore, it appears that the apical proteins, Crb and Sdt reciprocally regulate each other's apical localization in polarized epithelia. The proper apical localization of Crb, DaPKC and Sdt observed in *Rho1*^{K} homozygous embryos prior to gland invagination is likely due to the maternal contribution of Rho1. However, reduced levels of Rho1 due to zygotic loss of Rho1 function are insufficient to maintain these apical proteins during embryogenesis.

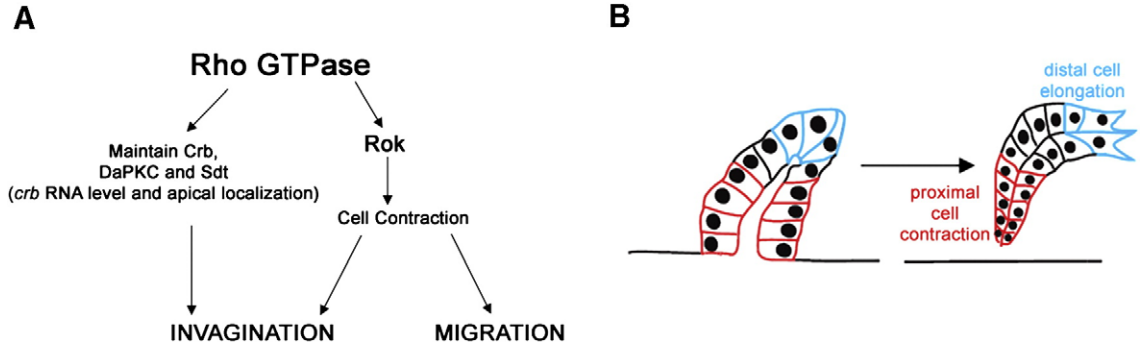

Fig. 8. Model for Rho1 function in salivary gland invagination and migration. During salivary gland invagination, Rho1 activity maintains Crb, DaPKC and Sdt in part by controlling *crb* RNA level and apical localization and induces apical constriction and cell shape change through Rok (A). Rho-Rok mediated cell constriction is also required for gland migration (A). Salivary gland turns posteriorly (B) through coordinated contraction and cohesive migration of proximal tip cells (B, red) and elongated motility of distal tip cells (B, blue). Diagrams are not drawn to scale.

The relevance of complete maintenance of A/B polarity during salivary gland invagination is reflected in *Drosophila* border cells that retain asymmetric distribution of polarity proteins during their migratory process (Pinheiro and Montell, 2004). One possible explanation for why it is necessary that gland epithelia maintain their apical polarity is that the glands are secretory organs that synthesize and secrete large quantities of digestive enzymes and glue proteins that allow the larva to attach to its environment. Thus, proper maintenance of all aspects of apical–basolateral polarity is likely to be essential for proper delivery of such secretory products into the lumen of the gland.

Integrin expression in the gland and CVM is necessary to initiate the posterior turn of the salivary gland (Bradley et al., 2003), possibly to mediate contact of the distal tip of the gland to the CVM; however, the contribution of the proximal gland cells to gland migration was previously not known. Here, we demonstrate that salivary gland cells, particularly those in the proximal half, contracted and migrated in a rounded type of motility and that these events were dependent on Rho1 function and downstream actin–myosin contraction. Our study provides novel evidence that the proximal gland cells play an active role in gland migration and do not passively follow the advancing distal tip. In fact, active contraction and cohesive migration of the proximal half of the gland allows the proximal tip of the gland to detach from the embryo's ventral surface and for the entire gland to turn and lie with its longest axis in the anterior–posterior direction.

Our studies reveal that migrating salivary glands have an advancing “front” that extends membrane protrusions and a contracting “back”. Moreover, expression of GFP reporter genes in subpopulations of gland cells indicates that distal and proximal gland cells largely retain their positions throughout gland migration. These features of salivary gland migration are in contrast to collective migration of border cells in the *Drosophila* ovary that do not have an apparent “back” and there is more fluidity within the cluster, with the position of the leading cells being interchangeable (Bianco et al., 2007; Prasad and Montell, 2007). One obvious distinction between salivary glands and border cells is that salivary glands have to coordinate cohesive migration of approximately 100 cells whereas border cells move as a cluster of six to ten cells. We propose that in large populations of migrating cells where cell positions are fixed, cohesive migration is best achieved if the front and back of the migrating group are well defined and each subpopulation contributes a unique role to the overall migration of the group. Consistent with this proposal, during wound healing of cultured epithelial sheets, cells several rows behind the wound edge extend lamellipodia suggesting an active role in collective migration of the sheet (Farooqui and Fenteany, 2005).

Our studies reveal that salivary glands use a unique combination of elongated motility at the distal tip and contractile motility at the proximal tip during their cohesive migration. A contractile versus elongated type of motility has previously been observed in tumor cells migrating in 3D matrices where the contractile or rounded type of motility was dependent on Rho signaling through ROCK, and the elongated type of motility was associated with Rac-dependent membrane protrusions and did not require Rho or ROCK (Sahai and Marshall, 2003). Thus, the salivary gland provides a unique model system not only for studying how cells migrate cohesively during embryogenesis but also for studying different modes of cell migration common to tumor cell migration.

Acknowledgments

We thank the Bloomington Stock Center, the Developmental Biology Hybridoma Bank, the Vienna Drosophila Research Center, the Rockefeller University Bio-imaging Center and our many colleagues for generously providing us with fly stocks and antisera, including S. Beckendorf, D. Bilder, A. Brand, N. Harden, E. Knust and N. Perrimon. We thank M. Schober, J. Zallen and members of the lab for critical reading of the manuscript. This work was supported by a Research Scholar Grant from the American Cancer Society to M.M.M.

Appendix A. Supplementary data

Supplementary data associated with this article can be found, in the online version, at doi:10.1016/j.ydbio.2008.06.007.

References

Alvarez, I., Navascues, J., 1990. Shaping, invagination, and closure of the chick embryo otic vesicle: scanning electron microscropic and quantitative study. Anat Rec 228, 315–326.
Barrett, K., Leptin, M., Settleman, J., 1997. The Rho GTPase and a putative RhoGEF mediate a signaling pathway for the cell shape changes in *Drosophila* gastrulation. Cell 91, 905–915.
Bianco, A., Poukkula, M., Cliffe, A., Mathieu, J., Luque, C., Fulga, T., Rorth, P., 2007. Two distinct modes of guidance signaling during collective migration of border cells. Nature 448, 362–365.
Bilder, D., Schober, M., Perrimon, N., 2003. Integrated activity of PDZ protein complexes regulates epithelial polarity. Nat Cell Biol 5, 53–58.
Bradley, P.L., Myat, M.M., Comeaux, C.A., Andrew, D.J., 2003. Posterior migration of the salivary gland requires an intact visceral mesoderm and integrin function. Dev Biol 257, 249–262.
Chihara, T., Kato, K., Taniguchi, M., NG, J., Hayashi, S., 2003. Rac promotes epithelial cell rearrangement during tracheal tubulogenesis in *Drosophila*. Development 130, 1419–1428.
Dawes-Hoang, R., Parmar, K., Christiansen, A., Phelps, C., Brand, A., Wieschaus, E., 2005. Folded gastrulation, cell shape change and the control of myosin localization. Development 132, 4165–4178.
Farooqui, R., Fenteany, G., 2005. Multiple rows of cells behind an epithelial wound edge extend cryptic lamellipodia to collectively drive cell-sheet movement. J Cell Sci 118, 51–63.
Grawe, F., Wodarz, A., Lee, B., Knust, E., Skaer, H., 1996. The *Drosophila* genes crumbs and stardust are involved in the biogenesis of adherens junctions. Development 122, 951–959.
Hardin, J., Keller, R., 1988. The behaviour and function of bottle cells during gastrulation of *Xenopus laevis*. Development 103, 211–230.
Henderson, K.D., Andrew, D.J., 2000. Regulation and function of *Scr*, *exd*, and *hth* in the *Drosophila* salivary gland. Dev Biol 217, 362–374.
Hilfer, S., 1983. Development of the eye of the chick embryo. Scan Elect Microsc 3, 1353–1369.
Horne-Badovinac, S., Bilder, D., 2008. Dynein regulates epithelial polarity and the apical localization of stardust A mRNA. PLoS Genet 4, e8.
Izaddoost, S., Nam, S.C., Bhat, M.A., Bellen, H.J., Choi, K.W., 2002. *Drosophila* crumbs is a positional cue in photoreceptor adherens junctions and rhabdomeres. Nature 416, 178–183.
Jaffe, A., Hall, A., 2005. Rho GTPases: biochemistry and biology. Annu Rev Cell Dev Biol 21, 247–269.
Klebes, A., Knust, E., 2000. A conserved motif in Crumbs is required for E-cadherin localisation and zonula adherens formation in *Drosophila*. Current Biology 10, 76–85.
Kolesnikov, T., Beckendorf, S., 2007. 18 Wheeler regulates apical constriction of salivary gland cells via the Rho-GTPase-signaling pathway. Dev Biol 307, 53–61.
Laufs, U., Liao, J., 1998. Post-transcriptional regulation of endothelial nitric oxide synthase mRNA stability by Rho GTPase. J Biol Chem 273, 24266–24271.
Lecaudey, V., Gilmour, D., 2006. Organizing moving groups during morphogenesis. Current Opinion in Cell Biology 18 107–107.
Lee, H.-H., Zaffran, S., Frasch, M., 2005. Muscle development in *Drosophila*. Springer, Berlin.
Lehmann, R., Tautz, D., 1994. *In situ* hybridization to RNA. Academic Press, San Diego.
Leptin, M., 1999. Gastrulation in *Drosophila:* the logic and the cellular mechanisms. EMBO J 18, 3187–3192.
Li, Z., Wang, L., Hays, T., Cai, Y., 2008. Dynein-mediated apical localization of crumbs transcript is required for Crumbs activity in epithelial polarity. J Cell Biol 180, 31–38.
Maeda, S., Matsuoka, I., Iwamoto, T., Kurose, H., Kimura, J., 2005. Down-regulation of Na+/Ca2+exchanger by Fluvastatin in rat cardiomyoblast H9c2 cells: involvement of RhoB in Na+/Ca2+exhanger mRNA stability. Mol Pharmacol 68, 320–414.
Magie, C., Meyer, M., Gorsuch, M., Parkhurst, S., 1999. Mutations in the Rho1 small GTPase disrupt morphogenesis and segmentation during early *Drosophila* development. Development 126, 5353–5364.
Magie, C., Parkhurst, S., 2005. Rho1 regulates signaling events required for proper Drosohila embryonic development. Dev Biol 278, 144–154.
Magie, C.R., Pinto-Santini, D., Parkhurst, S.M., 2002. Rho1 interacts with p120^{ctn} and a-catenin, and regulates cadherin-based adherens junction components in *Drosophila*. Development 129, 3771–3782.
Mikkola, M., Millar, S., 2006. The mammary bud as a skin appendage: unique and shared aspects of development. J Mammary Gland Biol Neoplasia 11, 187–203.
Mizuno, T., Amano, M., Kaibuchi, K., Nishida, Y., 1999. Identification and characterization of *Drosophila* homolog of Rho-kinase. Gene 238, 437–444.
Myat, M.M., 2005. Making tubes in the *Drosophila* embryo. Dev Dyn 232, 617–632.

Myat, M.M., Andrew, D.J., 2000a. Fork head prevents apoptosis and promotes cell shape change during formation of the *Drosophila* salivary glands. Development 127, 4217–4226.
Myat, M.M., Andrew, D.J., 2000b. Organ shape in the *Drosophila* salivary gland is controlled by regulated, sequential internalization of the primordia. Development 127, 679–691.
Myat, M.M., Andrew, D.J., 2002. Epithelial tube morphology is determined by the polarized growth and delivery of apical membrane. Cell 111, 879–891.
Nikolaidou, K., Barrett, K., 2004. A rho GTPase signaling pathway is used reiteratively in epithelial folding and potentially selects the outcome of Rho activation. Current Biology 14, 1822–1826.
Pellikka, M., Tanentzapf, G., Pinto, M., Smith, C., McGlade, C.J., Ready, D.F., Tepass, U., 2002. Crumbs, the *Drosophila* homologue of human CRB1/RP12, is essential for photoreceptor morphogenesis. Nature 416, 143–149.
Pinheiro, E., Montell, D.J., 2004. Requirement for Par-6 and Bazooka in *Drosophila* border cell migration. Development 131, 5243–5251.
Pirraglia, C., Jattani, R., Myat, M.M., 2006. Rac GTPase in epithelial tube morphogenesis. Developmental Biology 290, 435–446.
Prasad, M., Montell, D., 2007. Cellular and molecular mechanisms of border cell migration analyzed using time-lapse live-cell imaging. Developmental Cell 12, 997–1005.
Reuter, R., Panganiban, G.E.F., Hoffman, F.M., Scott, M.P., 1990. Homeotic genes regulate the spatial expression of putative growth factors in the visceral mesoderm of *Drosophila* embryos. Development 110, 1031–1040.
Sahai, E., Marshall, C., 2003. Differing modes of tumour cell invasion have distinct requirements for Rho/ROCK signalling and extracellular proteolysis. Nat Cell Biol 5, 711–719.
Schoenwolf, G., Smith, J., 1990. Mechanisms of neurulation: traditional viewpoint and recent advances. Development 109, 243–270.
Self, A., Paterson, H., Hall, A., 1993. Different structural organization of Ras and Rho effector domains. Oncogene 8, 655–661.
St Johnston, D., 2005. Moving messages: the intracellular localization of mRNAs. Nat Rev Mol Cell Biol 6, 363–375.
Tepass, U., Knust, E., 1990. Phenotypic and developmental analysis of mutations at the crumbs locus, a gene required for the development of epithelia in *Drosophila melanogaster*. Roux's Arch Dev Biol 199, 189–206.
Tepass, U., Knust, E., 1993. Crumbs and stardust act in a genetic pathway that controls the organization of epithelia in *Drosophlia melanogaster*. Developmental Biology 159, 311–326.
Winter, C., Wang, B., Ballew, A., Royou, A., Karess, R., Axelrod, J., Luo, L., 2001. *Drosophila* rho-associated kinase (Drok) links frizzled-mediated planar cell polarity signaling to the actin cytoskeleton. Cell 105, 81–91.
Woolner, S., Jacinto, A., Martin, P., 2005. The small GTPase Rac plays multiple roles in epithelial sheet fusion—Dynamic studies of *Drosophila* dorsal closure. Dev Biol 282, 163–173.